Adipose-derived mesenchymal stem cells ameliorate chronic experimental autoimmune encephalomyelitis

Journal:	*Stem Cells*
Manuscript ID:	SC-09-0489.R1
Manuscript Type:	Original Research
Date Submitted by the Author:	21-Jul-2009
Complete List of Authors:	Constantin, Gabriela; University of Verona, Dept of Pathology Marconi, Silvia; University of Verona, Dept. of Neurological Sciences Rossi, Barbara; Section of Pathology, Dept of Pathology Angiari, Stefano; Section of Pathology, Dept of Pathology Calderan, Laura; University of Verona, Department of Morphological-Biomedical Sciences Anghileri, Elena; University of Verona, Dept. of Neurological Sciences Gini, Beatrice; University of Verona, Dept. of Neurological Sciences Bach, Simone; University of Verona, Dept of Pathology Martinello, Marianna; University of Verona, Dept of Pathology Bifari, Francesco; University of Verona, Department of Clinical and Experimental Medicine Galie', Mirco; University of Verona, Department of Morphological-Biomedical Sciences Turano, Ermanna; University of Verona, Dept. of Neurological Sciences Budui, Simona; University of Verona, Dept of Pathology Sbarbati, Andrea; University of Verona, Department of Morphological-Biomedical Sciences Krampera, Mauro; University of Verona, Department of Clinical and Experimental Medicine Bonetti, Bruno; University of Verona, Dept. of Neurological Sciences
Keywords:	Adipose, Autoimmune disease, Cell adhesion molecules, Experimental models, In vivo optical imaging, Mesenchymal stem cells, Nervous system, Neural induction

Therapeutic efficacy of adipose MSC in chronic EAE

Adipose-derived mesenchymal stem cells ameliorate chronic experimental autoimmune encephalomyelitis

Gabriela Constantin,[1] Silvia Marconi,[2] Barbara Rossi,[1] Stefano Angiari,[1] Laura Calderan,[3] Elena Anghileri,[2] Beatrice Gini,[2] Simone Dorothea Bach,[1] Marianna Martinello,[1] Francesco Bifari,[4] Mirco Galiè,[3] Ermanna Turano[2], Simona Budui[1], Andrea Sbarbati,[3] Mauro Krampera, [4] Bruno Bonetti.[2]

[1]Department of Pathology, Section of General Pathology, University of Verona, Strada le Grazie 8, 37134 Verona, Italy;

[2]Department of Neurological Sciences and Vision, Section of Neurology, University of Verona, Policlinico G.B. Rossi, P.le L.A. Scuro, 10, 37134 Verona, Italy;

[3]Department of Morphological-Biomedical Sciences, Section of Anatomy, University of Verona, Strada le Grazie 8, 37134 Verona, Italy;

[4]Department of Clinical and Experimental Medicine, Section of Haematology, Policlinico G.B. Rossi, P.le L.A. Scuro, 10, 37134 Verona, Italy.

Author contribution:

Gabriela Constantin: Conception and design, Final approval of manuscript, Financial support, Manuscript writing

Silvia Marconi: Data analysis and interpretation

Barbara Rossi: Data analysis and interpretation

Stefano Angari: Data analysis and interpretation

Laura Calderan: Data analysis and interpretation

Elena Anghileri: Data analysis and interpretation

Beatrice Gini: Data analysis and interpretation

Simone Dorothea Bach: Data analysis and interpretation

Marianna Martinello: Data analysis and interpretation

Francesco Bifari: Provision of study material, Collection and/or assembly of data

Mirco Galiè: Provision of study material, Collection and/or assembly of data

Ermanna Turano: Data analysis and interpretation

Simona Budui: Data analysis and interpretation

Andrea Sbarbati: Conception and design, Manuscript writing

Mauro Krampera: Conception and design, Final approval of manuscript, Financial support

Bruno Bonetti: Conception and design, Final approval of manuscript, Financial support, Manuscript writing

Acknowledgements. This work was supported in part by grants from the National Multiple Sclerosis Society, New York, NY, USA (GC), Fondazione Cariverona (GC, BB, MK); Italian Ministry of Education and Research (BB), Fondazione Italiana Sclerosi Multipla (FISM), (GC, BB).

Key words: adipose-derived MSC; chronic EAE; immune regulation; neural precursors; T lymphocytes; in vivo imaging; growth factors.

Please address correspondence to:

Bruno Bonetti, MD, PhD
Associate Professor in Neurology
Section of Clinical Neurology
Department of Neurological Sciences and Vision
University of Verona
P.le L.A. Scuro 10
37134 Verona, Italy
Phone +39-045-8124694
Fax+39-045-8027492
e-mail: bruno.bonetti@univr.it

Gabriela Constantin, MD, PhD
Assistant Professor of Pathology
Section of General Pathology
Department of Pathology
University of Verona
Strada le Grazie 8
37134 Verona, Italy
+39-045-8027102
+39-045-8027127
gabriela.constantin@univr.it

Abstract

Mesenchymal stem cells (MSC) represent a promising therapeutic approach for neurological autoimmune diseases; previous studies have shown that treatment with bone marrow-derived MSC induces immune modulation and reduces disease severity in experimental autoimmune encephalomyelitis (EAE), an animal model of multiple sclerosis. Here we show that intravenous administration of adipose-derived MSC (ASC) before disease onset significantly reduces the severity of EAE by immune modulation and decreases spinal cord inflammation and demyelination. ASC preferentially home into lymphoid organs, but migrates also inside the CNS. Most importantly, administration of ASC in chronic established EAE significantly ameliorates the disease course and reduces both demyelination and axonal loss, and induce a Th2-type cytokine shift in T cells. Interestingly, a relevant subset of ASC expresses activated α4 integrins and adheres to inflamed brain venules in intravital microscopy experiments. Bioluminescence imaging shows that α4 integrins control ASC accumulation in inflamed CNS. Importantly, we found that ASC cultures produce basic fibroblast growth factor, brain-derived growth factor and platelet-derived growth factor-AB. Moreover, ASC infiltration within demyelinated areas is accompanied by increased number of endogenous oligodendrocyte progenitors. In conclusion, we show that ASC have clear therapeutic potential by a bimodal mechanism, by suppressing the autoimmune response in early phases of disease as well as by inducing local neuro-regeneration by endogenous progenitors in animals with established disease. Overall our data suggest that ASC represent a valuable tool for stem cell-based therapy in chronic inflammatory diseases of the CNS.

INTRODUCTION

Multiple sclerosis and its animal model, the experimental autoimmune encephalomyelitis (EAE), are autoimmune disorders targeting the CNS, where the inflammatory response leads to demyelination (1). In both diseases, axonal pathology occurs in the early phase, correlates with inflammation and critically contributes to disease severity (1-3). Thus, chronic EAE is a suitable model to test therapeutic approaches which target simultaneously both inflammation and neuro-degeneration. In this regard, neural precursor cells (NPC) were the first candidates for cell-based therapy in neuro-inflammation because of their capacity of cell replacement in chronic EAE, as well as their local and systemic immune modulatory effects in relapsing EAE (4, 5). In fact, NPC were effective when injected after disease stabilization in chronic EAE animals by promoting neuro-regeneration through a supportive effect on endogenous progenitors (4). The homing of NPC into the CNS was dependent on integrin VLA-4, the counter-ligand for endothelial VCAM-1 (5).

However, the invasiveness associated with harvesting of NPC and the reduced number of cells that can be obtained may limit their clinical application. As the efforts to bring experimental advances to the clinic are mounting, the source of these cells is becoming a crucial issue. A potential alternative to NPC is represented by mesenchymal stem cells (MSC) (also named multipotent stromal cells) (6), a subset of adult stem cells present in virtually all tissues, including bone marrow (BM), adipose tissue, umbilical cord blood, dermis (7-9). MSC can differentiate *in vitro* into multiple mesenchymal and non-mesenchymal lineages and can efficiently induce the proliferation, migration and differentiation of neural endogenous progenitors through the secretion of neural growth factors, thus representing an attractive therapy for regenerative medicine (10). In addition, MSC have relevant immune modulatory effects both *in vivo* and *in vitro*, as they can suppress many functions of immune cells (11-14). This feature makes MSC suitable for the

therapy of autoimmune diseases. Indeed, mouse BM-MSC have been shown to ameliorate chronic and relapsing EAE (15-19), by inhibiting Th1 T cells and modulating Th17-polarized response (13, 20). However, the beneficial effect was evident only when BM-MSC were injected before or at the onset of disease, whereas they were unable to cure established disease (15). More recently, human BM-MSC have been shown not only to induce Th2-shift of the immune response, but also to promote endogeneous repair in chronic EAE (19). However, the mechanisms of BM-MSC contribution to neuro-regeneration in chronic EAE are not clearly understood. In fact, murine BM-MSC do not express α4 integrins (21), and the study of BM-MSC homing in EAE lesions has provided conflicting results regarding the capacity of BM-MSC to migrate into the inflamed CNS (15-19).

In the last years much attention has been paid to adipose-derived MSC (ASC), because adipose tissue is an abundant, easily accessible and appealing source of donor tissue for autologous cell transplantation (22, 23). Several groups have demonstrated that ASC display multi-lineage plasticity *in vitro* and *in vivo* (for review see 23). In addition, MSC have a much higher frequency in the adipose tissue (about 500 fold more) than in BM (22, 23). Although both cell populations share many common biological features, certain key differences in surface marker expression between BM-MSC and ASC were detected (24, 25). For instance, while both express the β1 chain of integrins (CD29), only ASC express CD49d (α 4 integrin) (20, 26), which forms a heterodimer with CD29 to create very late activation antigen-4 (VLA-4). This is very interesting in light of the key role of the interaction between VLA-4 and VCAM-1 in the migration of cells into the inflamed CNS in EAE/MS (27). Finally, several groups including ours have found evidence for neural trans-differentiation of ASC in vitro (28-36), a property which may be relevant for neuroregeneration.

Here we show that the preventive administration of ASC ameliorated chronic EAE by a dual mechanism, one involving the systemic immune modulation on autoreactive T cells (with a

consequent reduction of spinal cord inflammation and demyelination) and one inducing local neurogenesis in inflamed spinal cord, through the secretion of neural growth factors. Most interestingly, ASC were effective in ameliorating chronic EAE even when administered after disease stabilization leading to the reduction of CNS inflammation, demyelination and axonal damage, as well as the increase of endogenous oligodendrocyte precursors.

MATERIALS AND METHODS

EAE induction and treatment protocols

Chronic EAE was induced in 6-8 weeks old C57Bl/6 female mice purchased from Harlan Italy (S. Pietro di Natisone, Italy), by subcutaneous immunization with 200 µg of MOG_{33-35} peptide in incomplete Freud's adjuvant containing 0.8 mg/ml Mycobacterium Tuberculosis, as previously described (37). Pertussis Toxin (50ng; Sigma Aldrich, Milan, Italy) was injected at the day of immunization and after 48 hrs. Body weight and clinical score were blindly registered according to a standard 0-5 scale: 0=healthy, 1=limp tail, 2=ataxia and/or paresis of hindlimbs, 3= paraplegia, 4= paraplegia with forelimb weakness or paralysis, 5=moribund or death animal. All animals were housed in pathogen-free conditions. The experiments received authorization from the Italian Ministry of Health, and were conducted following the principles of the NIH Guide for the Use and Care of Laboratory Animals, and the European Community Council (86/609/EEC) directive. To evaluate the clinical and pathological efficacy of ASC in chronic EAE, cells were administered with two distinct protocols: preventive and therapeutic. In the preventive setting, ASC (either from wild type mice or from animals transgenic for GFP) were injected intravenously (iv) at 3 and 8 days post-immunization (dpi), i. e. before the disease onset. In the therapeutic protocol, ASC were administered iv after the peak of disease severity, when the clinical score was stable (23 and 28 dpi). For each injection, $1x10^6$ MSC were resuspended in 1 ml of PBS without Ca^{2+} and Mg^{2+} and injected through the tail vein; each iv administration was divided in two injections of $0.5X10^6$ ASC in 0.5ml vehicle. Control mice received only vehicle.

Mesenchymal stem cell cultures

Murine ASC were obtained from 6-8 weeks old C57Bl/6J mice, as well as from C57Bl/6-Tg(UBC-GFP)30Scha/J mice expressing the GFP fluorescent protein. The isolation of stromal-vascular fraction from adipose tissue was carried out on 10 ml of minced samples

obtained from subcutaneous abdominal fat tissue, as previously described (36). Briefly, after washing in HBSS, extracellular matrix was digested at 37°C with collagenase, centrifuged at 1200g and the pellet was resuspended in NH_4Cl; the stromal fraction was then collected by centrifugation and filtration. Murine BM-MSC were collected by flushing femurs and tibias with medium and filtered as previously described (11, 35). Cells were then cultured in DMEM, glucose, GLUTAMAX I™, 15% heat-inactivated adult bovine serum, penicillin and streptomycin (Invitrogen Corp. Carlsbad, CA). After 72 hrs, non-adherent cells were removed. When 70-80% adherent cells were confluent, they were trypsinized, harvested and expanded by using culture medium with 50ng/ml HB-EGF (R&D System, Minneapolis, MN). All the experiments were performed using MSC at 17-23 passages.

MSC immune phenotyping and adhesion molecules expression

Murine MSC were recognized by immune phenotype using mAbs specific for CD106 (VCAM-1), CD9, CD44, CD80, CD138 and Sca1. In addition, the absence of haematopoietic markers (CD45, CD11c and CD34) and endothelial markers (CD31) was assessed as previously described (11). All mAbs were purchased from Pharmigen/Becton Dickinson (Palo Alto, CA, USA). We also assessed the expression of PDGFα R on ASC with a polyclonal antiserum (Sigma), followed by biotinylated secondary anti-goat IgG and Streptavidin-PE. For the study of adhesion molecule expression, ASC were labelled with fluorescent antibodies for α4 integrins (PS/2 clone, kindly provided by Dr. Eugene Butcher, Stanford University), LFA-1 (anti-αL-chain; clone TIB213 from American Type Culture Collection/ATCC, VA, USA), PSGL-1 (clone 4RA10, kindly provided by Dr. Dietmar Vestweber, Max Plank Institute, Germany), L-selectin (Mel-14 clone, ATCC) and CD44 (IM/7 clone, ATCC). Isotype-matched antibodies were used as controls. For immune phenotypic analysis, MSC were detached using trypsin/EDTA (Sigma), washed and

resuspended at 10^6 cells/ml. Cell suspension was incubated with 15% adult bovine serum, followed by incubation with the specific mAbs at 4°C for 30 min. At least 10,000 events were analyzed by flow cytometry (FACScalibur, Becton Dickinson) using the Cell Quest software.

ImageStream data acquisition and analysis

ASC were prepared for immunostaining as described above and then incubated with 10 μg/ml of anti-α4 integrins mAb for 30 min on ice. After washing, cells were stained with goat anti-rat IgG-PE conjugated (Caltag Laboratories). Stained cells were re-suspended in PBS and images were acquired on the ImageStream® imaging cytometer System 100 (Amnis Corporation, Seattle, WA, USA). Images of fixed cells were collected and analyzed using ImageSteam Data Exploration and Analysis Software (IDEAS) (38). α4 integrin clustering was evaluated analyzing the distribution on the cells surface of the fluorescence pattern. Uniform (uniform distribution of fluorescence), Clustered (small spots of fluorescence) and Caps (big clusters of fluorescence) cells were gated using the Area feature vs the Delta Centroid XY feature (39). The area feature was calculated for channel 4 (PE-specific emission; area of fluorescence), applying to the images a previously created Threshold mask; this feature allowed us to discriminate between cells with larger fluorescence area (high area values) and smaller fluorescence area. The Delta Centroid (DC) XY feature calculates the distance between the center of the PE fluorescence image and the center of the brightfield image for each image pair. This feature distinguished images with globally distributed staining (lower DC values) from those with capped staining (higher DC values). When plotted versus the Area feature, DC XY permits to distinguish between punctate and uniform staining (39). Cells with Area values higher than 600 and Radial Delta Centroid values lower than 16 were considered “Uniform”; cells with Area values lower than 600 and Radial Delta Centroid values lower than 16 were considered

"Clustered" (small spots of fluorescence). Cells with Radial Delta Centroid values higher than 16 were considered "Caps" cells (highly polarized fluorescence).

Proliferation assays

MOG_{35-55} activated T cells were obtained from draining lymph nodes of mice immunized with antigen as previously described (37). $CD4^+$ T cells ($2x10^5$/well) were co-cultured with 5,000, 2,000 and 1,000 irradiated ASC in 96-well microtiter plates in the presence of 30 μg/ml antigen peptide and $8x10^5$ APC (irradiated splenocytes) for 3 days. [^{3}H] thymidine (1mCi) was added in each well 18hrs before the end of cultures. [^{3}H] thymidine uptake was determined in a Microplate Scintillation Counter and expressed as counts per minute (CPM). In separate experiments we studied the *ex vivo* proliferation of T cells from peripheral lymph node cells isolated from mice immunized with MOG_{35-55} peptide and treated or not with ASC. Total draining lymph node cells were isolated both from mice treated with ASC in the pre-clinical phase of disease (3 and 8 dpi) and from mice receiving ASC after disease stabilization (at 23 and 28 dpi). For all *ex vivo* proliferation experiments, $1x10^6$ cells/well were cultured in 96-well microtiter plates in the presence of 10-30 μg/ml MOG peptide or 1 μg/ml anti-CD3 plus 2 μg/well anti-CD28mAb. After 72 hrs of incubation, cultures were pulsed for 18 hrs with 1 μCi per well of [H^3]-thymidine, and proliferation was measured from triplicate cultures.

Bio-Plex and ELISA assays for cytokines and growth factors

Supernatants from lymph node cells isolated from mice treated with ASC in the pre-clinical phase of disease or after disease stabilization, or derived from in vitro co-cultures between MOG_{35-55} activated T cells and ASC were used for Bioplex cytokine assays (BioRad), following the manufacturer's instructions. Briefly, anti-cytokine conjugated beads were plated in 96-well microtiter plates and then removed by vacuum filtration. Samples were

then added, and the plate was incubated for 30 min by mixing at 300 rpm. Bio-Plex cytokine assays were sequentially incubated with the detection antibody and streptavidin-PE; samples were then analyzed immediately by a Bioplex array-system. Unknown cytokine concentrations were automatically calculated by Bio-Plex software using a standard curve derived from a recombinant cytokine standard. To determine the production by ASC of basic fibroblast growth factor (bFGF), brain-derived growth factor (BDNF), ciliary neurotrphic factor (CNTF) and platelet-derived growth factor (PDGF) AB, supernatants were obtained from ASC ($3x10^4$) in basal condition and after incubation with TNFα (50U/ml) for 24 hrs and analyzed by Quantikine® ELISA Immunoassay (R&D), following the manufacturer's instructions. Briefly, cells were grown in 24-well plates and the supernatants were harvested and centrifuged for 10 min to remove cell debris. Samples were added in 96-well pre-coated plates and incubated for 2 hrs at RT. After washing, a specific polyclonal antibody followed by substrate solution were added and the colour development was measured at 450nm (BioRad Microplate Reader). The concentration of growth factors was calculated using the standard curve.

Cell transfection and biolumiscence in vivo imaging

Murine ASC were transiently transfected with a plasmid encoding for the firefly luciferase (*Photinus pyralis*), under the control of the SV40 early enhancer/promoter region (pGL4.13 internal control vector; Promega Corporation, USA). Transfection was performed by lipofection with the Lipofectamine^{TM} 2000 reagent system (Invitrogen), according with the manufacture's instructions; cells were transfected in a 12 well plate ($6x10^5$ cells/well) and the Lipofectamine (μl)/DNA (μg) ratio used was 2.5/1. After lipofection, cells were washed and kept for 18 hrs at 37°C in complete medium. The transfection efficiency was evaluated transfecting with the same protocol ASC with a plasmid encoding for eGFP, under the control of a CMV promoter (pEGFP-N1 vector; Clontech). Cells were analyzed by flow

cytometry for the eGFP fluorescence: efficiency was always higher than 55% in all the experiments. The day after transfection, 1.2 x10^6 ASC were transplanted iv into healthy or EAE mice (7 to 9 days after disease onset). For anti-α4 integrin treatment, mice were injected iv with 500 μg of anti-α4-integrin mAb every other day, whereas cells were incubated before transplantation with 100 μg anti-α4 mAb in 200 μl PBS, for 30 min on ice. Bioluminescent signal generated by luciferase activity was measured using the In Vivo Imaging System IVIS® 200 (Xenogen Corporation, USA). An aqueous solution of the luciferase substrate D-luciferin (150 mg/kg; Xenogen) was injected iv 12 min before imaging. Animals were under general anesthesia (2.5% isoflurane in oxygen). Images were acquired using a CCD camera (acquisition time: 6 min) and analyzed with the Living Image 2.6 software and the Living Image 3D (Xenogen). A pseudo-color image representing light intensity (blue, least intense; red, most intense) was created for each mouse.

Intravital microscopy

ASC were labelled with green 5-chloromethylfluorescein diacetate (CMFDA; Molecular Probes, Eugene, OR). To mimic brain inflammation in early phase of EAE, C57Bl/6 female mice were injected i.p. with 12 μg of LPS (*Escherichia coli* 026:B6; Sigma-Aldrich) 5–6 hrs before the intravital experiment (5, 40). Previous studies have shown that LPS or TNF administration induces expression of VCAM-1 as well as expression of other adhesion molecules in brain vessels mimicking endothelial activation during EAE (5, 40). Briefly, animals were anesthetized and the preparation was placed on an Olympus BX50WI microscope and a water immersion objective with long focal distance (Olympus Achroplan) was used. A total of 1x10^6 fluorescent labelled cells/condition was slowly injected into the carotid artery by a digital pump. The images were visualized by using a silicon-intensified video camera (VE-1000 SIT; Dage MTI) and recorded using a digital VCR. ASC that remained stationary on venular wall for > 30 s were considered adherent.

Histology and immunohistochemistry

Frozen sections were obtained from brain, lumbar, dorsal and cervical spinal cord and processed for hematoxylin and eosin, Spielmeyer stainings and immunohistochemistry to evaluate the presence of inflammatory cells, demyelination, axonal loss and oligodendrocyte progenitors, according to standard protocols and as previously described (41, 42). For immunohistochemistry, primary antibodies for macrophages/monocytes, CD3, CD4, CD8 T cells (Serotec, Oxford, UK), neurofilaments (Chemicon, Temecula, CA) or PDGFα R (Sigma) were used. In order to evaluate the tissue distribution and the differentiation by GFP^+ ASC, sections were stained with DAPI and then with anti-CD11b (R&D), CD3, GFAP (Dako), O4 (Chemicon) or PDGFα R mAbs overnight (42, 43). Slides were viewed under Leica TCS SP5 confocal scanner. See Supplementary data for further details concerning the immunohistochemical procedures.

Statistical analysis

Statistical analysis using a two-tailed Student's *t*-test was performed to evaluate differences between ASC-treated and control conditions for several parameters: T cell proliferation, cytokine production, pathological alterations and number of oligodendrocyte progenitors in EAE lesions.

RESULTS

Preventive administration of ASC reduces the severity of chronic EAE

1. Clinical and neuropathological effects of ASC-based therapy

Control mice developed the first clinical signs of EAE at (mean ± SD) 12.7 ± 1.3 dpi, reached a peak at 14.0 ± 1.2 dpi and then presented a stable disease course, typical of this chronic model (Figure 1A and Table 1). The pathological analysis of spinal cord sections in all control mice showed the presence of demyelinated areas and inflammatory infiltrates, composed of T lymphocytes and monocyte/macrophages (Supplementary Figure 1). Mice treated with ASC showed a drastic reduction of the mean clinical scores at disease peak (1.1 ± 0.7 versus 2.5 ± 0.7 in control mice; $p<0.002$) (Table 1), as well as of the areas of inflammation, demyelination and axonal loss at 50 dpi (Table 1; Supplementary Figure 1). GFP^+ ASC had similar clinical and pathological effects on EAE as compared to wild type ASC (data not shown). No anti-GFP autoreactivity was detected in the serum from ASC-treated EAE animals by performing immunocytochemistry on GFP^+ ASC cultures (Supplementary Figure 1). In addition, no evidence of GFP reactivity was seen in $CD11b^+$ macrophages in all EAE lesions examined with both treatment protocols (data not shown).

2. Mechanisms of the beneficial effects of the preventive treatment with ASC in EAE

2a. Immune regulation

In agreement with previous results (14), we found that ASC also inhibited MOG-specific T lymphocyte proliferation both *in vitro* and *ex vivo*. In fact, ASC co-cultured *in vitro* with $CD4^+$ T cells in the presence of MOG_{35-55} peptide exerted a dose-dependent inhibition of T cell proliferation and induced a significant decrease of IFNγ (Supplementary Figure 2), GM-CSF, IL-17, IL-4 and IL-5 production (data not shown). No effect was observed on the

production of TNFα and IL-1β, which were produced in low amounts after stimulation in vitro with MOG (data not shown). Interestingly, we observed a selective increase of IL-10 production (Supplementary Figure 2), suggesting that ASC promote the generation of T lymphocytes with regulatory activity *in vitro*. We next asked whether the effects observed *in vitro* were also responsible for the *in vivo* activity of ASC. *Ex vivo* analysis of peripheral lymph node cells isolated from mice treated with ASC showed a significant reduction of proliferation in the presence of MOG_{35-55}, when compared to control mice (Figure 1). In addition, the production of both pro-inflammatory and anti-inflammatory cytokines by peripheral lymph node cells isolated from mice treated with ASC and stimulated with MOG_{35-55} was generally suppressed in comparison with control EAE animals (Figure 1).

2b. ASC and local neurogenesis in EAE lesions

GFP^+ ASC distributed in normal mice mainly in the spleen and lymph nodes; by contrast, in EAE mice ASC displayed an increased migration to lymphoid organs but also penetrated into the spinal cord (Figure 2A), where they persisted up to 93 dpi. In basal conditions, a very limited number of ASC was found in the sub-meningeal spaces of both brain and spinal cord (data not shown). In spinal cord from mice with EAE the vast majority of ASC was detected mainly within the lesions (Figure 2 C-F); only few GFP^+ ASC were observed either in regions of normal appearing white matter.

We then assessed whether ASC could favor remyelination and regeneration when administered in the pre-clinical phase of disease. Given the relevance of the PDGF pathway in both oligodendrogenesis and MSC self-renewal (44, 45), we first assessed by flow cytometry the expression of PDGFα R on ASC cultures and found that 28% of them displayed PDGFα R (Supplementary Figure 3). We found that ASC treatment induced local neurogenesis by inducing a three-fold increase of PDGFα R^+ oligodendrocyte progenitors (15.0 ± 2.1), when compared to untreated mice (5.4 ± 1.1). We then asked whether the

increase in oligodendrocyte progenitors derived from local precursors or from PDGFα R^+ ASC penetrated in the spinal cord. In this regard, the comparative analysis between the total number of PDGFα R^+ cells and the number of GFP^+/PDGFα R^+ ASC showed that about 40% of oligodendrocyte precursors derived from ASC (Figures 2A and 2B), a proportion similar to that found in culture. We next investigated whether GFP^+ ASC migrated in the parenchyma underwent mature glial differentiation. As summarized in Figure 2B, the double staining with glial phenotypic markers showed that a very limited subset of GFP^+ ASC displayed mature glial differentiation markers (i. e. GFAP or O4) in EAE lesions. No evidence of binucleated GFP^+ cells expressing such markers was observed in all samples examined (data not shown). Thus, these results suggest that ASC penetrated and persisted into inflamed spinal cord, where they contributed to activate oligodendroglial progenitors. To better support this point, we then assessed by ELISA assay the secretion by ASC of growth factors, which may influence their self-renewal as well as the process of oligodendrogenesis. As summarized in Figure 2G, we found that ASC both in basal conditions and after TNF-α stimulation produced detectable amounts of bFGF, PDGF-AB and BDNF; no production of CNTF was observed in any condition (data not shown).

Therapeutic administration of ASC ameliorates the severity of chronic EAE

1. Clinical and neuropathological effects

We then assessed whether ASC had an effect when injected after the disease entered the chronic phase and the disability is stable. Surprisingly, and in contrast with the results obtained with murine BM-MSC (14), we found that therapeutic administration of ASC at 23 and 28 dpi significantly ameliorated the disease severity (Figure 3, Table 1). The effect was clinically significant at 41 dpi and increased progressively until 72 dpi. The pathological

analysis at sacrifice confirmed the beneficial effect of ASC, in terms of reduction of both demyelination and inflammation (Figure 3; Table 1). Strikingly, axonal density in spinal cord of ASC-treated animals was almost comparable to normal mice (Table 1).

2. Mechanisms of the beneficial effects of the therapeutic treatment of EAE with ASC

2a. Immune regulation

The therapeutic effect of ASC on established EAE induced us to seek for their underlying mechanisms of action. Interestingly, homing of ASC into lymph nodes was lower in mice receiving cells after the disease onset, when compared to animals treated in the pre-clinical phase of disease. In fact, the number of ASC injected with the therapeutic protocol detected in lymph nodes was only two times higher than that observed in healthy mice (Figure 4A) and about five times lower than mice receiving ASC in the pre-clinical phase of disease (Figure 2A). The proliferation of MOG-specific T cells and the production of pro-inflammatory cytokines was not different between mice groups at 72 dpi (Figure 4B). However, basal production of IFNγ by T cells was increased in mice treated with ASC (Figure 4C). Importantly, we observed an enhanced production of cytokines IL-4, IL-5 and IL-10 by T cells (Figure 4D), suggesting that ASC injected in mice with established disease induce a shift towards a Th2 phenotype contributing to disease amelioration.

2b. ASC homing to CNS and induction of local neurogenesis in EAE lesions

In addition to lymphoid organs, the analysis of the distribution of GFP^+ ASC in spinal cord from EAE mice sacrificed at 72 dpi confirmed the ability of these cells to home into the inflamed CNS when injected in mice with established disease. In this regard, their distribution pattern and quantity (10.1 ± 2.2 GFP^+ cells/mm^2 in EAE lesions) were comparable to those observed with the preventive protocol. To explore the mechanisms sustaining the homing of ASC to inflamed CNS we evaluated their adhesion molecule

profile. Flow cytometry analysis revealed that α4 integrins were expressed on up to 25% of ASC, whereas BM-MSC have no expression of these integrins (Supplementary Figure 3), as previously reported (20, 26). These results, together with previous data showing that MSC express β1 integrins, suggest that ASC express VLA-4 (α4β1) integrin. Moreover, ImageStream analysis revealed that 92% of VLA-4$^+$ cells express activated VLA-4 (Figure 5A, B). To assess their ability to interact with inflamed brain endothelium, we performed intravital microscopy experiments in an experimental model in which brain endothelium expresses high levels of VCAM-1, the endothelial ligand for VLA-4 integrin (35). The results obtained confirmed that ASC were able to efficiently adhere to inflamed brain vessels in vivo (Fig. 5C). To definitively demonstrate that ASC accumulate in the inflamed brain through a VLA-4-dependent mechanism, we transfected ASC with luciferase and performed bioluminescence *in vivo* assay. The results showed that ASC accumulate preferentially in spleen and liver in healthy mice, but significantly migrated also into inflamed CNS of EAE mice, with preferential accumulation in lumbo-sacral spinal cord (Fig 5D). Interestingly, anti-α4 integrin antibody dramatically inhibited ASC accumulation in inflamed CNS (Figure 5D).

We next sought for the mechanisms responsible for the therapeutic effect of ASC. We first evaluated the number of oligodendrocyte precursors, which may contribute to neuro-regeneration. As observed in mice receiving ASC during the pre-clinical phase of EAE, ASC penetration in EAE lesions induced a three-fold increase of the total number of PDGFα R$^+$ cells, when compared to EAE lesions from control mice (Figure 6A). The comparative analysis of the total number of PDGFα R$^+$ cells and of GFP$^+$/PDGFα R$^+$ ASC showed that about 20% of oligodendrocyte precursors derived from ASC (a proportion similar to that expressing PDGFαR on ASC before injection, Supplementary Figure 3), whereas the majority originated from local precursors (Figures 6A-C). As shown also for

mice treated in the pre-clinical phase of disease, we observed that a very limited number of GFP^+ cells expressed the markers of mature glial cells (i. e. GFAP or O4) (Figure 6D, E); in particular, mature oligodendrocyte derived from ASC were less than 2%, suggesting that ASC do not significantly contribute directly to the process of remyelination. As in preventively ASC-treated mice, no evidence of binucleated GFP^+ cells expressing such markers was observed in all samples examined (data not shown).

DISCUSSION

Stem cells are a promising approach for the treatment of autoimmune diseases of the CNS due to their immune modulatory effects and neuro-regenerative potential. NPC seems to represent the gold standard in chronic EAE, because of their ability to penetrate into the CNS, where they display high neuro-regenerative properties as well as anti-inflammatory effects (4, 5). However, the source and availability of stem cells is becoming a crucial issue for their clinical application. In this regard, previous studies have shown that BM-MSC were effective in ameliorating both chronic and relapsing-remitting EAE (15, 17, 18). However, the beneficial effect in chronic EAE was evident only when murine BM-MSC were injected before the disease onset (15). In both experimental conditions, the main mechanism was related to the immune-suppression exerted by murine BM-MSC on autoreactive B and T cells (15,17, 24, 25), while their effects within the inflamed CNS are still a matter of debate (15-18). More recently, also human BM-MSC have been shown to be effective on chronic EAE, by inducing Th2-polarized immune response, reducing IFN-γ and Th17 producing cells and promoting oligodendrogenesis and inhibiting astrogliosis in EAE (19). Interestingly, recent data show that BM-MSC inhibit key mechanisms responsible for EAE induction by a paracrine conversion of CCL2 chemokine from agonist to antagonist of the Th17 cell function (20). However, although promising results have been previously obtained with BM-MSC, the invasive nature of BM biopsies may limit their practicality for wider clinical applications. It has been estimated that the frequency of ASC in collagenase-digested adipose tissue is about 500-fold higher that in freshly isolated BM cells (22, 23). Moreover, the most important features of adipose tissue as a cell source might be the relative expandability of this tissue and the consequent ease with which it can be obtained in relatively large quantities with minimal risk (22).

In the present paper we show that ASC have a significant beneficial effect on chronic EAE not only when administered in the pre-clinical phase of disease, but also when injected after disease entered an irreversible clinical course, thus displaying a true therapeutic effect. In both cases, the amelioration of clinical scores was accompanied by a strong reduction of spinal cord inflammation as well as of demyelination and axonal damage in EAE lesions. Our results show that these cells exerted their beneficial effects by acting simultaneously in two distinct sites: lymphoid organs and inflamed CNS. Similarly to BM-MSC, ASC induced dramatic changes on antigen-specific T cells in vitro, with dose-dependent inhibition of proliferation and modulation of cytokine secretion (15, 17). We show that the time of ASC administration is crucial for their homing capacity to lymph nodes with potential implications for the mechanisms of diseases inhibition. The migration to lymph nodes was significantly higher when ASC were administered shortly after the induction of the autoimmune response, whereas it was lower when administered in mice with established disease. This difference may explain the anti-proliferative effect and broad inhibition of both pro- and anti-inflammatory cytokine production observed when ASC were injected in the pre-clinical phase of disease, but not in mice with established disease. Interestingly, we provided evidence that ASC injected in mice with established disease induced a Th2-type shift of antigen-specific CD4 T cells in lymph nodes supporting recent results obtained with human BM-MSC in chronic EAE (19).

The knowledge of the molecular mechanisms controlling ASC-based therapy is of critical importance in the perspective of potential future applications of ASC in humans. The characterization of the molecular mechanisms involved in the immune modulation and those sustaining ASC homing into the CNS during EAE/MS represent an important contribution to the understanding of ASC tissue-specific delivery. However, the mechanisms involved in the migration of MSC (of any origin) into the brain are largely unknown. In addition to their immune modulatory activity shared with BM-MSC, our results

suggest that the beneficial effect of ASC on chronic EAE relies also on the ability to penetrate into the inflamed CNS, due to the expression on a significant ASC subset of activated $\alpha4\beta1$ integrin, a key adhesion molecule involved in leukocyte and stem cell migration into the inflamed CNS (5, 46). We demonstrated the presence on a subset of ASC of activated $\alpha4$ integrin, which mediated the interaction with inflamed brain endothelium, as shown by intravital microscopy experiments. Moreover, bioluminescence in vivo assay showed that ASC display $\alpha4$ integrin-dependent migration in inflamed CNS, suggesting that adipose tissue may represent a valuable source of stem cells able to cross BBB and exert their action into the inflamed CNS.

The analysis of distribution of GFP^+ ASC in EAE mice injected either before or after disease onset indicates that these cells penetrated in the inflamed spinal cord and persisted there up to three months, thus suggesting long-lasting effects in target tissues. The persistence of ASC up to 75 days after i.v. injection has been already described in previous studies (47). In our model, chronic inflammation and expression of VCAM-1 on brain endothelium in MOG-induced EAE may help to continuously recruit ASC expressing $\alpha4$ integrin from the blood. In addition to promote homing, we speculate that chronic inflammation together with the secretion of growth factors might be responsible also for the prolonged survival of ASC in inflamed spinal cord. These cells in fact produce in basal conditions and after stimulation with TNF-α bFGF and PDGF-AB, two factors known to promote MSC self-renewal (48). In addition to ASC, activated microglia present in active EAE lesions are also known to produce bFGF (49). From these observations, it is conceivable that the local inflammatory environment supports the prolonged survival of ASC within EAE lesions.

We then asked whether and how ASC could have a neuro-regenerative effect in EAE spinal cord. In this regard, ASC may participate to remyelination by either differentiating into mature oligodendrocytes able to form new myelin or indirectly by promoting the survival

and proliferation of endogenous precursors cells. A direct participation of ASC to remyelination seems unlikely, since the proportion of GFP^+ cells expressing PDGFα R in EAE lesions of both protocols was comparable to that observed in ASC cultures before injection. Another evidence pledging against a direct neuro-regenerative effect of ASC came from the analysis of the markers of mature glia expressed by ASC *in situ*, which revealed that only a very limited proportion of GFP^+ ASC acquired the phenotype of mature oligodendroglial cells. In particular, less than 2% of $O4^+$ oligodendrocytes derived from ASC at all time points investigated, a proportion that probably do not significantly contribute to the process of remyelination. Although we did not observe any binucleated GFP^+ cells expressing markers of mature glia in our samples, we were not able to establish whether the expression of neural markers on such limited ASC sub-population in EAE spinal cord reflected a process of true differentiation towards a glial phenotype or rather derived from a process of cell fusion, as seen in other experimental conditions (50).

Overall, our results indicate that the main mechanism responsible for the neuro-regenerative effect in chronic EAE is a robust activation of endogenous progenitors in EAE lesions, which probably accounted for the process of remyelination. Indeed, the number of endogenous oligodendrocyte precursors (GFP^-/PDGFα R^+) was significantly higher in ASC-treated animals in comparison to control EAE. Regarding the molecular mechanism involved in the cross-talk between ASC and oligodendroglial precursors, MSC are known to produce a variety of neurotrophic factors with relevant effects on NPC proliferation, migration and differentiation (10, 51-53). Here we show that ASC are able to secrete bFGF, PDGF-AB and BDNF, all factors strongly supporting the process of oligodendrogenic differentiation. In fact, a key role for these factors in the amelioration of EAE observed in our experiments is also suggested by two studies in which the delivery of bFGF or BDNF induced a beneficial effect of clinical and pathological scores in EAE together with increase of mature oligodendrocyte and their progenitors in EAE model (54, 55).

In conclusion, our results show that ASC produce a beneficial effect in chronic EAE by a bimodal mechanism, through suppression of the autoimmune response in early phases of disease and promotion of Th2-polarized immune response as well as through the induction of local neuro-regeneration by endogenous progenitors in animals with established disease. Our data show that ASC have relevant therapeutic potential in an animal model of chronic MS and might represent a valuable tool for stem cell-based therapy in chronic inflammatory diseases of the CNS. The persistence of ASC in EAE lesions, together with the beneficial effect displayed in the therapeutic protocol in chronic EAE, when clinical and pathological signs are irreversible, may have important implications for the future therapeutic use of ASC also in other chronic, non-inflammatory CNS diseases, where the recruitment of local progenitors is warranted.

REFERENCES

1. Raine CS. The neuropathology of multiple sclerosis. In: Raine CS, McFarland H, Tourtellotte W, eds. *Multiple sclerosis*. London, UK: Chapman & Hall Med, 1997:149-172.
2. Brex PA, Ciccarelli O, O'Riordan JI et al. A longitudinal study of abnormalities on MRI and disability from multiple sclerosis. **N ENGL J MED** 2002;346:158-164.
3. Trapp BD, Peterson J, Ransohoff RM et al. Axonal transection in the lesions of multiple sclerosis. **N ENGL J MED** 1998;338:278–285.
4. Pluchino S, Quattrini A, Brambilla E et al. Injection of adult neurospheres induces recovery in a chronic model of multiple sclerosis. **NATURE** 2003;422:688-694.
5. Pluchino S, Zanotti L, Rossi B et al. Neurosphere-derived multipotent precursors promote long-lasting neuroprotection by an immunomodulatory mechanism. **NATURE** 2005;436:266-271.
6. Horwitz EM, Le Blanc K, Dominici M et al. Clarification of the nomenclature for MSC: the International Society for Cellular Therapy position statement. **CYTOTHERAPY** 2005;7:393-395.
7. Erices A, Conget P, Minguell JJ. Mesenchymal progenitor cells in human umbilical cord blood. **BR J HAEMATOL** 2000;109:235–242.
8. Jiang Y, Vaessen B, Lenvik T et al. Multipotent progenitor cells can be isolated from postnatal murine bone marrow, muscle, and brain. **EXP HEMATOL** 2002;30:896–904.
9. Zuk PA, Zhu M, Mizuno H et al. Multilineage cells from human adipose tissue: implications for cell-based therapies. **TISSUE ENG** 2001;7: 211–228.
10. Munoz JR, Stoutenger BR, Robinson AP et al. Human stem/progenitor cells from bone marrow promote neurogenesis of endogenous neural stem cells in the hippocampus of mice. **PROC NATL ACAD SCI USA** 2005;102:18171-18176.
11. Krampera M, Glennie S, Dyson J. Bone marrow mesenchymal stem cells inhibit the

response of naive and memory antigen-specific T cells to their cognate peptide. **BLOOD** 2003;101:3722-3729.

12. Uccelli A, Moretta L, Pistoia V. Immunoregulatory function of mesenchymal stem cells. **EUR J IMMUNOL** 2006;36:2566-2573.
13. Uccelli A, Moretta L, Pistoia V. Mesenchymal stem cells in health and disease. **NAT REV IMMUNOL** 2008;8:726-736.
14. Cui L, Yin S, Liu W et al. Expanded adipose-derived stem cells suppress mixed lymphocyte reaction by secretion of prostaglandin E2. **TISSUE ENG** 2007;13:1185-1195.
15. Zappia E, Casazza S, Pedemonte E et al. Mesenchymal stem cells ameliorate experimental autoimmune encephalomyelitis inducing T-cell anergy. **BLOOD** 2005;106:1755-1761.
16. Zhang J, Li Y, Chen J et al. Human bone marrow stromal cell treatment improves neurological functional recovery in EAE mice. **EXP NEUROL** 2005 ;195:16-26.
17. Gerdoni E, Gallo B, Casazza S et al. Mesenchymal stem cells effectively modulate pathogenic immune response in experimental autoimmune encephalomyelitis. **ANN NEUROL** 2007;61:219-227.
18. Kassis I, Grigoriadis N, Gowda-Kurkalli B Et al. Neuroprotection and immunomodulation with mesenchymal stem cells in chronic experimental autoimmune encephalomyelitis. **ARCH NEUROL** 2008;65:753-761.
19. Bai L, Lennon DP, Eaton V et al. Human bone marrow-derived mesenchymal stem cells induce Th2-polarized immune response and promote endogenous repair in animal models of multiple sclerosis. **GLIA** 2009 [Epub ahead of print].
20. Rafei M, Campeau PM, Aguilar-Mahecha A et al. Mesenchymal stromal cells ameliorate experimental autoimmune encephalomyelitis by inhibiting CD4 Th17 T cells in a CC chemokine ligand 2-dependent manner. **J IMMUNOL** 2009;182:5994-6002.
21. De Ugarte DA, Alfonso Z, Zuk PA et al. Differential expression of stem cell mobilization-

associated molecules on multi-lineage cells from adipose tissue and bone marrow. **IMMUNOL LETT** 2003;89:267–270.

22. Fraser JK, Wulur I, Alfonso Z et al. Fat tissue: an underappreciated source of stem cells for biotechnology. **TRENDS BIOTECHNOL** 2006;24:150-154.
23. Parker AM, Katz AJ. Adipose-derived stem cells for the regeneration of damaged tissues. **EXPERT OPIN BIOL THER** 2006;6:567-578.
24. Puissant B, Barreau C, Bourin P et al. Immunomodulatory effects of human adipose tissue-derived stem cells: comparison with bone marrow mesenchymal stem cells. **BR J HAEMATOL** 2005;129:118-129.
25. McIntosh K, Zvonic S, Garrett S et al. The immunogenicity of human adipose-derived cells: temporal changes in vitro. **STEM CELLS** 2006;24: 1246-1253.
26. Gronthos S, Franklin DM, Leddy HA, et al. Surface protein characterization of human adipose tissue-derived stromal cells. **J CELL PHYSIOL** 2001;189:54-63.
27. Constantin G, Majeed M, Giagulli C et al. Chemokines trigger immediate beta2 Integrin affinity and mobility changes: differential regulation and roles in lymphocyte arrest under flow. **IMMUNITY** 2000;16:759-769.
28. Safford KM, Hicok KC, Safford SD et al. Neurogenic differentiation of murine and human adipose-derived stromal cells. **BIOCHEM BIOPHYS RES COMMUN** 2002;294:371-379.
29. Safford KM, Safford SD, Gimble JM et al. Characterization of neuronal/glial differentiation of murine adipose-derived adult stromal cells. **EXP NEUROL** 2004;187:319-328.
30. De Ugarte DA, Morizono K, Elbarbary A et al. Comparison of multi-lineage cells from human adipose tissue and bone marrow. **CELLS TISSUES ORGANS** 2003;174:101–109.
31. Kang SK, Shin MJ, Jung JS et al. Autologous adipose tissue-derived stromal cells for treatment of spinal cord injury. **STEM CELLS DEV** 2006;15:583-594.

32. Kokai LE, Rubin JP, Marra KG. The potential of adipose-derived adult stem cells as a source of neuronal progenitor cells. **PLAST RECONSTR SURG** 2005;116:1453-1460.

33. Fujimura J, Ogawa R, Mizuno H et al. Neural differentiation of adipose-derived stem cells isolated from GFP transgenic mice. **BIOCHEM BIOPHYS RES COMMUN** 2005;333:116-121.

34. Ning H, Lin G, Lue TF et al. Neuron-like differentiation of adipose tissue-derived stromal cells and vascular smooth muscle cells. **DIFFERENTIATION** 2006 ;74:510-518.

35. Krampera M, Marconi S, Pasini A et al. Induction of neural-like differentiation in human mesenchymal stem cells derived from bone marrow, fat, spleen and thymus. **BONE** 2007;40:382-390.

36. Anghileri E, Marconi S, Pignatelli A et al. Neuronal differentiation potential of human adipose-derived mesenchymal stem cells. **STEM CELLS DEV** 2008;17:909-916.

37. Constantin G, Laudanna C, Brocke S et al. Inhibition of experimental autoimmune encephalomyelitis by a tyrosine kinase inhibitor. **J IMMUNOL** 1999;162:1144-1149.

38. George TC, Fanning SL, Fitzgeral-Bocarsly P et al. Quantitative measurement of nuclear translocation events using similarity analysis of multispectral cellular images obtained in flow. **J IMMUNOL METHODS** 2006;311:117-125.

39. Bolomini-Vittori M, Montresor A, Giagulli C et al. Regulation of conformer-specific activation of the integrin LFA-1 by a chemokine-triggered Rho signaling module. **NAT IMMUNOL** 2009;10:185-94.

40. Piccio L, Rossi B, Scarpini E et al. Molecular mechanisms involved in lymphocyte recruitment in brain microcirculation: critical roles for PSGL-1 and trimeric G alpha-linked receptors. **J IMMUNOL** 2002;168:1940-1949.

41. Lovato L, Cianti R, Gini B et al. Transketolase and CNPase I are specifically recognized by IgG autoantibodies in multiple sclerosis patients. **MOL CELL PROTEOMICS** 2008;7:2337-2349.

42. Lolli F, Mulinacci B, Carotenuto A et al. An N-glucosylated peptide detecting disease-specific autoantibodies, biomarkers of multiple sclerosis. **Proc Natl Acad Sci USA** 2005;102:10273-10278.

43. Bonetti B, Pohl J, Gao YL et al. Cell death during autoimmune demyelination: effector but not target cells are eliminated by apoptosis. **J Immunol** 1997;159:5733-5741.

44. Tokunaga A, Oya T, Ishii Y et al. PDGF receptor beta is a potent regulator of mesenchymal stromal cell function. **J Bone Mineral Res** 2008;23:1519-1528

45. Lachapelle F, Avellana-Adalid V, Nait-Oumesmar B, Baron-Van Evercooren A. Fibroblast growth factor-2 and platelet-derived growth factor AB promote adult SVZ-derived oligodendrogenesis in vivo. **Mol Cell Neurosci** 2002;20:390-403

46. Yednock TA, Cannon C, Fritz LC et al. Prevention of experimental autoimmune encephalomyelitis by antibodies against alpha 4 beta 1 integrin. **Nature** 1992;356:63-66.

47. Meyerrose TE, De Ugarte DA, Hofling AA, et al. In vivo distribution of human adipose-derived mesenchymal stem cells in novel xenotransplantation models. **Stem Cells** 2007;25:220-227.

48. Zaragosi LE, Ailhaud G, Dani C. Autocrine fibroblast growth factor 2 signaling is critical for self-renewal of human multipotent adipose-derived stem cells. **Stem Cells** 2006;24:2412-2419.

49. Liu X, Mashour GA, De Webster H, Kurtz A. Basic FGF and FGF receptor 1 are expressed in microglia during experimental autoimmune encephalomyelitis: temporally distinct expression of midkine and pleiotrophin. **Glia** 1998;24:390-397.

50. Spees JL, Olson SD, Ylostalo J et al. Differentiation, cell fusion and nuclear fusion during ex vivo repair of epithelium by human adult stem cells from bone marrow stroma. **Proc Natl Acad Sci USA** 2003;100:2397-2402.

51. Caplan A, Dennis JE. Mesenchymal stem cell as trophic mediators. **J CELL BIOCHEM** 2006;98:1076-1084.

52. Rivera FJ, Couillard-Despres S, Pedre X et al. Mesenchymal stem cells instruct oligodendrogenic fate decision on adult neural stem cells. **STEM CELLS** 2006;24:2209-2219.

53. Goddard DR, Berry M, Butt AM. In vivo actions of fibroblast growth factor 2 and insulin-like growth factor I on oligodendrocyte development and myelination in the central nervous system. **J NEUROSCI RES** 1999;57:74-85.

54. Ruffini F, Furlan R, Poliani PL et al. Fibroblast growth factor 2 gene therapy reverts the clinical course and the pathological signs of chronic experimental autoimmune encephalomyelitis in C57BL/6 mice. **GENE THERAPY** 2001;8:1207-1213.

55. Makar TK, Bever CT, Singh IS et al. Brain-derived neurotrophic factor gene delivery in an animal model of multiple sclerosis using bone marrow stem cells as a vehicle. **J NEUROIMMUNOL** 2009;210:40-51.

Figure legends

Figure 1. Preventive administration of ASC inhibits clinical signs of EAE and reduces proliferation and cytokine production of T cells *ex vivo*. A. Mice were treated with ASC (■) or saline (Control) (●) during the pre-clinical phase (3 and 8 dpi). Daily mean of the clinical scores shows a statistical difference between the two groups of mice starting from 14 dpi. The results from the same experiment are also summarized in Table 1. **B**. Total draining lymph node cells were isolated from mice transplanted with ASC in the pre-clinical phase of the disease and from control mice. *Ex vivo* analysis of T cell proliferation of lymph node cells ($1x10^6$) after stimulation with the MOG_{35-55} peptide or soluble anti-CD3/anti-CD28 mAbs clearly showed a significant reduction of [^{3}H]-thymidine incorporation in T lymphocytes obtained from mice treated with ASC, in comparison to control (CTRL) EAE animals. Data were obtained from 5 mice/condition. **C**, **D**. Cytokine production was also modulated in lymph node cells obtained from mice treated with ASC before disease onset and showed a general suppression of cytokine production, in comparison to controls ($p<0.02$).

Figure 2. Distribution and differentiation of ASC injected during the pre-clinical phase of disease. A. The distribution of GFP$^+$ ASC injected iv at 3 and 8 dpi was assessed in lymphoid organs and spinal cord of healthy animals (after 14 days) and EAE mice at several time points. **B.** The fate of ASC injected iv was assessed by immunofluorescence in the spinal cord of healthy and EAE mice, by evaluating the number of GFP$^+$ cells expressing the glial phenotypic markers GFAP for astrocytes, O4 for mature oligodendrocytes and PDGFα R for oligodendroglial precursors. **C, D**. Confocal microscope image with DAPI (blue), CD3 (red) and GFP (green) showing the presence of GFP$^+$ ASC in perivascular cuffs in EAE spinal cord at 16 (**C**) and 30 dpi (**D**). **E, F**. GFP$^+$ ASC are detected in white matter spinal cord at 93 dpi. **G.** The concentration of bFGF, BDNF and

PDGF-AB has been analyzed by ELISA assay in the supernatants of ASC stimulated (w TNF) or not (w/o TNF) with 50U/ml TNF-α. Data are expressed as mean ± SD from three different experiments.

Figure 3. Administration of ASC in mice with established EAE ameliorates disease course. A. Mice were treated with ASC (■) or vehicle (Control) (●) during the chronic phase of disease (23 and 28 dpi). Daily mean of the clinical scores shows that after about two weeks ASC-treated animals displayed a significant amelioration of the clinical course in comparison to control EAE mice. Hematoxylin and eosin (**B**, **C)** and Spielmeyer (**D, E**) stainings of lumbar spinal cords confirmed that clinical amelioration was accompanied by a significant reduction of both inflammation and demyelination in ASC-treated animals (**C, E**) in comparison to control mice (**B, D**). Quantification of these results is summarized in Table 1. **F**, **G**. Immunohistochemistry on lumbar spinal cord sections for PDGFα R shows an increase of oligodendrocyte precursors in EAE lesions from ASC-treated mice (**G**), as compared to control animals (**F**).

Figure 4. Distribution and functional analysis *ex vivo* of peripheral lymph node cells isolated from mice treated with ASC during established disease. A. Quantification of GFP^+ ASC in lymphoid organs from mice treated with ASC injected at 23 and 28 dpi. Although significantly higher than in healthy mice ($p<0.04$), note the low number of cells in the lymph node in comparison to those observed in EAE animals treated with the preventive protocol (Figure 4A). **B.** The proliferation of lymph node cells isolated from these mice was not significantly different from control EAE animals. Data were obtained from 9 mice/condition. **C**. Cytokine contents in supernatants of lymph node cells showed that basal production of IFNγ was increased in cells obtained from mice treated with ASC. **D.** Interestingly, we observed an enhanced production ($p<0.02$) of IL-4, IL-5 and IL-10 by T

cells both in the absence and in the presence of antigen, suggesting that ASC injected in mice with established disease induced a shift towards a Th2 phenotype.

Figure 5. α4 integrin controls ASC migration into the CNS in EAE mice. A, B. ASC were stained with anti-α4 integrin antibody followed by anti-rat IgG-PE. Analysis of α4 integrin clustering was evaluated by analyzing the distribution on the cells surface of the fluorescence: Uniform (uniform distribution of fluorescence), Clustered (small spots of fluorescence) and Caps (big clusters of fluorescence). Images of eight representative cells are shown in **A**: brightfield (BF; white), darkfield/side scatter (SSC; blue), α4-integrin (VLA-4-PE; red). **B**. Quantification of the three different populations of ASC, according with α4 integrin clustering on their surface shows that the vast majority of ASC display functionally active α4 integrin. **C**. A micrograph showing fluorescently labelled ASC arrested in inflamed brain venules in intravital microscopy experiments. Cells are the bright intravascular dots (arrows) inside blood vessels labelled with fluorescent dextrans. **D**. ASC transfected with the luciferase reporter gene were transplanted iv in healthy or EAE mice (7 to 9 days after disease onset). Bioluminescent signal by luciferase activity generated by transfected ASC in transplanted mice was visualized by the IVIS® 200 imaging system, 7 days after ASC injection. Images show the bioluminescent signal detected in one representative animal per group (left: healthy mouse; middle: EAE; right: EAE + anti-α4 integrin antibody). The colour scale next to the images indicates the signal intensity, with red and blue representing high and low signal intensity, respectively. In healthy animals, iv injection of ASC results in their accumulation in liver and spleen, whereas in EAE mice the bioluminescent signal is prevalent in areas corresponding to dorsal-lumbar spinal cord; noteworthy, the pre-treatment with anti-α4 integrin mAb dramatically reduced the signal in these areas.

Figure 6. Differentiation of ASC injected during established disease. A. The number of PDGFα R$^+$ cells in EAE lesions was significantly increased in animals treated with ASC with the therapeutic protocol, in comparison to controls at 72 dpi. **B.** The study of the expression of glial markers on GFP$^+$ cells in EAE lesions indicate that a subset of ASC penetrated into the spinal cord expressed PDGFα R$^+$, but only a very limited number of ASC acquired the phenotype of mature GFAP$^+$ astrocytes or O4$^+$ oligodendrocytes. In EAE spinal cord from mice injected with GFP$^+$ ASC at 23 and 28 dpi, a subset of GFP$^+$ cells (green, **C$_1$**) express PDGFα R (red **C$_3$**), as evident in merge image (**C** and **inset**); nuclei are stained with DAPI (blue, **C$_2$**). In consecutive sections, we show examples of GFP$^+$ cells (**D$_2$**, **E$_2$**) expressing the markers of mature oligodendrocytes expressing O4 (**D$_3$**) or GFAP$^+$ astrocytes (**E$_3$**), as visible in merge images (**D**, **E**); DAPI staining in **D$_1$** and **E$_1$**.

Bonetti et al Figure 1

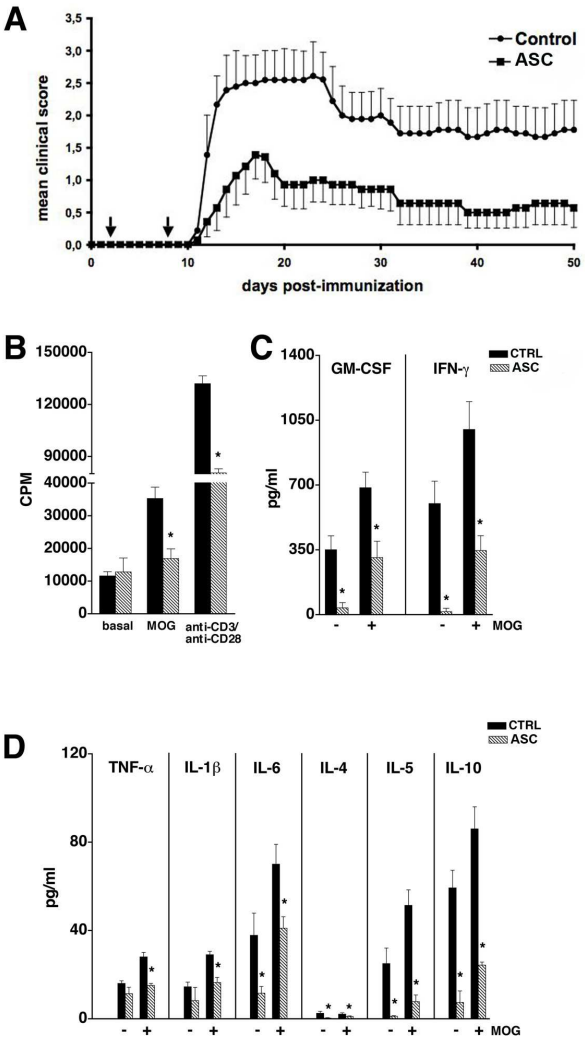

Bonetti et al Figure 2

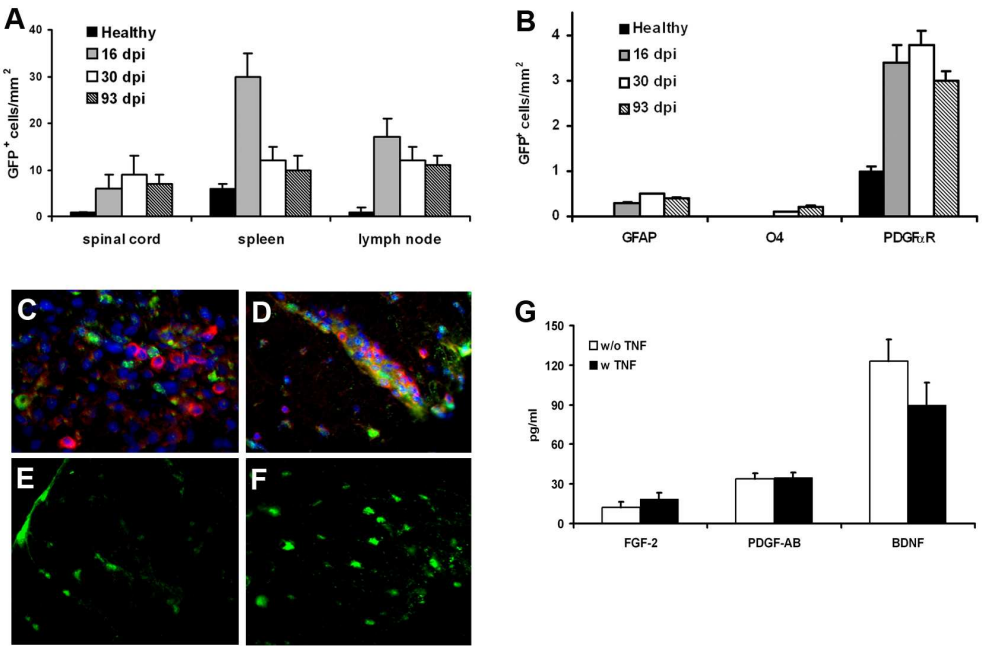

Bonetti et al Figure 3

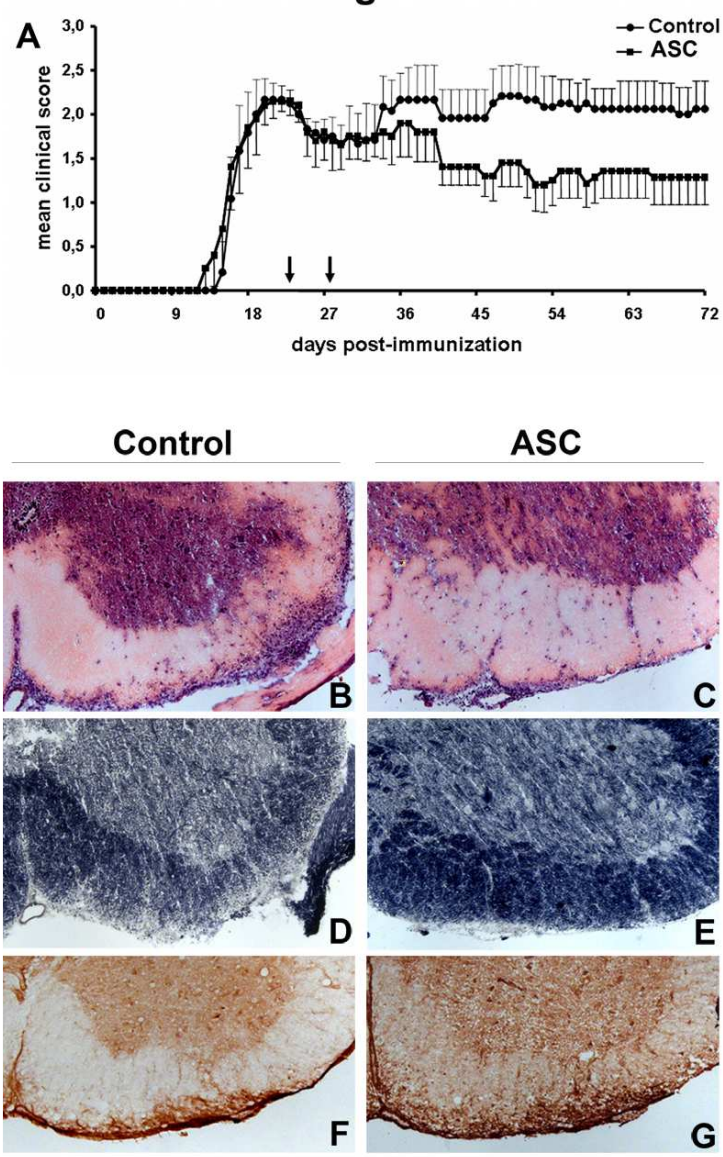

Bonetti et al **Figure 4**

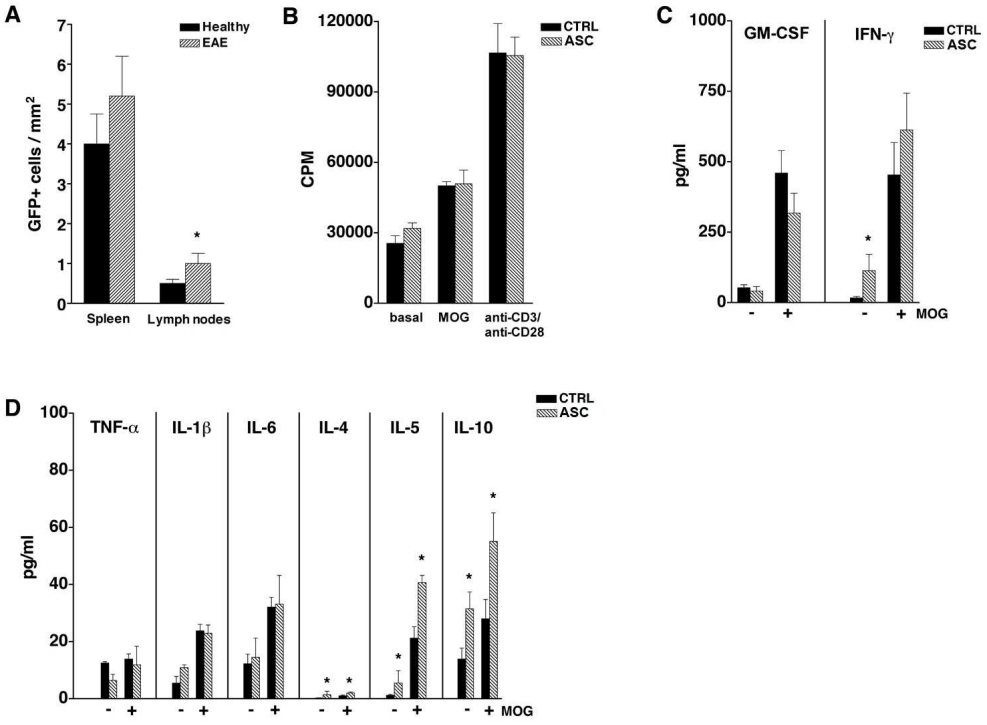

149x130mm (254 x 254 DPI)

Bonetti et al Figure 5

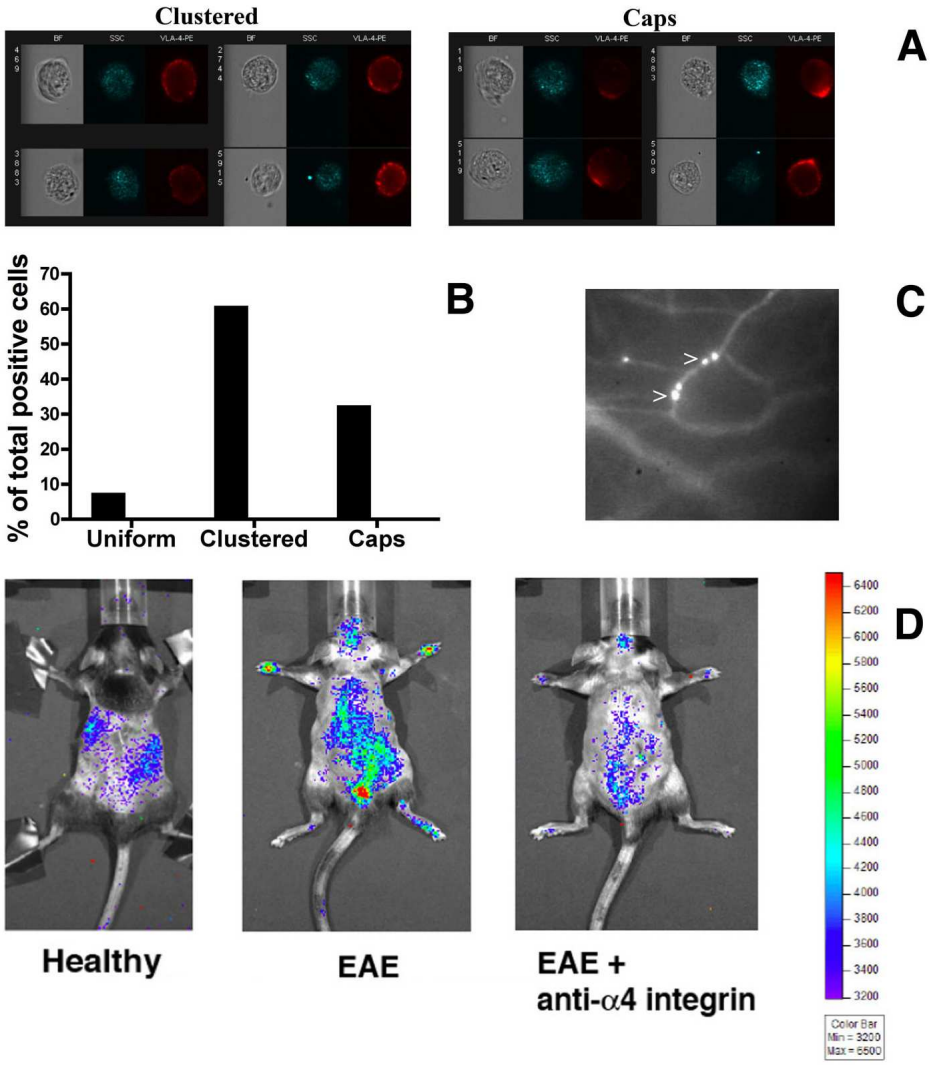

Bonetti et al Figure 6

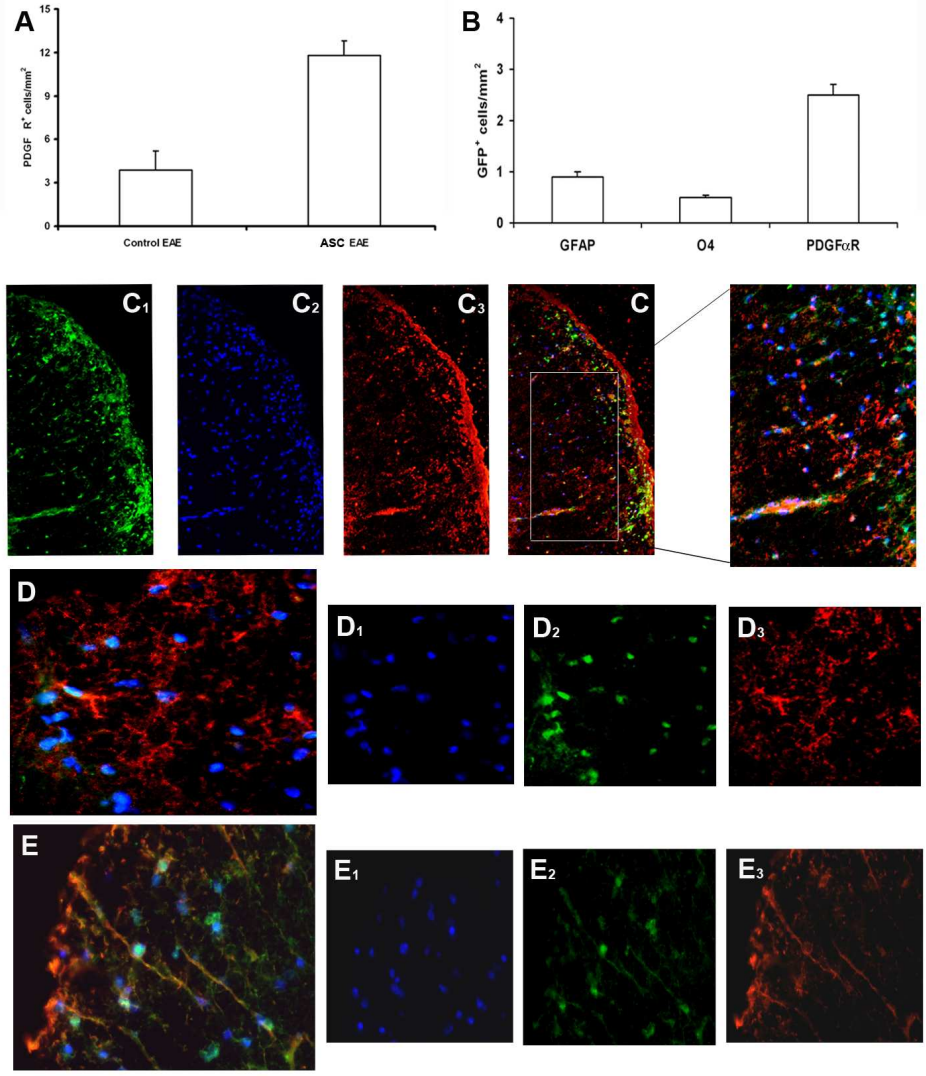

Table 1. Clinical and pathological features of EAE mice treated with ASC with preventive (top) and therapeutic (bottom) treatment protocols

Preventive Treatment (nr. animals)	Disease onset (dpi)	Mean maximum score	Mean cumulative Score	Inflammatory Area (%)[a]	Demyelinated Area (%)[a]	Axonal Loss (%)[b]
Control (10)[c]	12.7 ± 1.3	2.5 ± 0.7	77.9 ± 36.2	18.9 ± 9.5	17.7 ± 8.5	21.8 ± 4.0
ASC (10)[c]	13.7 ± 2.1	1.1 ± 0.7*	32.8 ± 21.7*	8.4 ± 7.7**	9.1 ± 7.6**	9.2 ± 5.1**

Therapeutic Treatment (nr. animals)	Mean maximum score	Mean cumulative Score (0-28 dpi)	Mean cumulative Score (29-72 dpi)	Inflammatory Area (%)[b]	Demyelinated Area (%)[b]	Axonal Loss (%)[c]
Control (10)[d]	2.2 ± 0.4	25.2 ± 5.3	92.2 ± 25.1	14.2 ± 6.9	14.6 ± 6.6	22.6 ± 6.0
ASC (10)[d]	2.3 ± 0.4	24.8 ± 6.5	63.0 ± 29.6*	7.7 ± 2.3*	7.1 ± 3.1*	3.9 ± 1.1***

[a] % of the total spinal cord section. [b] % of axonal loss in demyelinated lesions in comparison to normal white matter.

[c] pathological changes refer to animals sacrificed at 50 dpi. [d] pathological changes refer to animals sacrificed at 72 dpi.

* $p < 0.002$. ** $p < 0.0005$. *** $p < 0.02$.

Supplementary Materials and Methods

ImageStream data acquisition and analysis

ASC were prepared for immunostaining as described above and then incubated with 10 μg/ml of anti-α4 integrins mAb for 30 min on ice. After washing, cells were stained with goat anti-rat IgG-PE conjugated (Caltag Laboratories). Stained cells were re-suspended in PBS and images were acquired on the ImageStream® imaging cytometer System 100 (Amnis Corporation, Seattle, WA, USA). Images of fixed cells were collected and analyzed using ImageSteam Data Exploration and Analysis Software (IDEAS) (33). α4 integrin clustering was evaluated analyzing the distribution on the cells surface of the fluorescence pattern. Uniform (uniform distribution of fluorescence), Clustered (small spots of fluorescence) and Caps (big clusters of fluorescence) cells were gated using the Area feature vs the Delta Centroid XY feature (34). The area feature was calculated for channel 4 (PE-specific emission; area of fluorescence), applying to the images a previously created Threshold mask; this feature allowed us to discriminate between cells with larger fluorescence area (high area values) and smaller fluorescence area. The Delta Centroid (DC) XY feature calculates the distance between the center of the PE fluorescence image and the center of the brightfield image for each image pair. This feature distinguished images with globally distributed staining (lower DC values) from those with capped staining (higher DC values). When plotted versus the Area feature, DC XY permits to distinguish between punctate and uniform staining (34). Cells with Area values higher than 600 and Radial Delta Centroid values lower than 16 were considered “Uniform”; cells with Area values lower than 600 and Radial Delta Centroid values lower than 16 were considered “Clustered” (small spots of fluorescence). Cells with Radial Delta Centroid values higher than 16 were considered “Caps” cells (highly polarized fluorescence).

Intravital microscopy

To mimic brain inflammation in early phase of EAE, C57Bl/6 female mice were injected i.p. with 12 µg of LPS (*Escherichia coli* 026:B6; Sigma-Aldrich) 5–6 hrs before the intravital experiment (40). Briefly, animals were anesthetized and the preparation was placed on an Olympus BX50WI microscope and a water immersion objective with long focal distance (Olympus Achroplan) was used. A total of $1x10^6$ fluorescent labelled cells/condition was slowly injected into the carotid artery by a digital pump. The images were visualized by using a silicon-intensified target video camera (VE-1000 SIT; Dage MTI) and a Sony SSM-125CE monitor and recorded using a digital VCR (Panasonic NV-DV10000). ASC that remained stationary on venular wall for 30 s were considered adherent.

Histology and immunohistochemistry

Histological assessment of spinal cord demyelination (Spielmeyer) and inflammatory infiltrates (H&E) in lumbo-sacral segments was blindly performed calculating affected areas in at least three sets (100 µm apart) of six sections for each animal. For immunohistochemistry, primary antibodies for macrophages/monocytes, CD3, CD4, CD8 T cells (Serotec, Oxford, UK), neurofilaments (Chemicon, Temecula, CA) or PDGFα R (Sigma) were incubated overnight. After washing, anti-rat biotinylated secondary antibody was added; the reaction was visualized with ABC kit (Vector Laboratories, Burlingame, CA) and diaminobenzidine (Sigma). Images of immune-peroxidase were obtained with Zeiss Axiophot microscope and Axiocam camera with Axiovision software. Lesions were identified on digital images of Spielmeyer-stained or H&E sections; the lesion area was determined following a manual outline of the lesion border and expressed as percentage of the total spinal cord section area. For the determination of axonal loss, the number of neurofilament-reactive profiles was manually counted within the lesions (on sections adjacent to Spielmeyer-stained section) and their density was calculated by dividing the

manual counts by the lesion area. The assessment of neural precursors was performed by counting the number of PDGFα R^+ cells on eight random 40X fields in the entire spinal cord section. In order to evaluate the tissue distribution, the relationship with inflammation and the differentiation by GFP^+ ASC in lymphoid organs and in spinal cord, sections were incubated with DAPI and then with anti-CD11b (R&D), CD3, GFAP (Dako), O4 (Chemicon) or PDGFα R mAbs overnight (42, 43); the signal was then detected by appropriate secondary biotinylated antibodies and Streptavidin Texas Red (Vector). We then assessed whether the administration of GFP^+ ASC induced the formation of anti-GFP antibodies that may influence the disease; for this purpose, GFP^+ ASC were incubated overnight with the serum (dilution 1:50) from control EAE and ASC-treated (both with preventive and therapeutic protocols) mice and the signal detected with anti-mouse biotinylated Ig and Streptavidin Texas Red (Vector). Slides were viewed under a Zeiss MC80 microscope or Leica TCS SP5 tandem confocal scanner with acquisition of images at different wave-length (DAPI 455nm, GFP 509nm, Texas Red 615nm). The proportion of GFP^+ MSC undergoing neural differentiation was calculated by dividing the number of GFP^+ MSC expressing neural phenotypic markers by the total number of GFP^+ MSC in lesion areas. All the above counts were performed in three sets (four sections 100 μm apart) for each animal. All data are expressed as mean percentage ± SD.

Bonetti et al Supplementary Figure 1

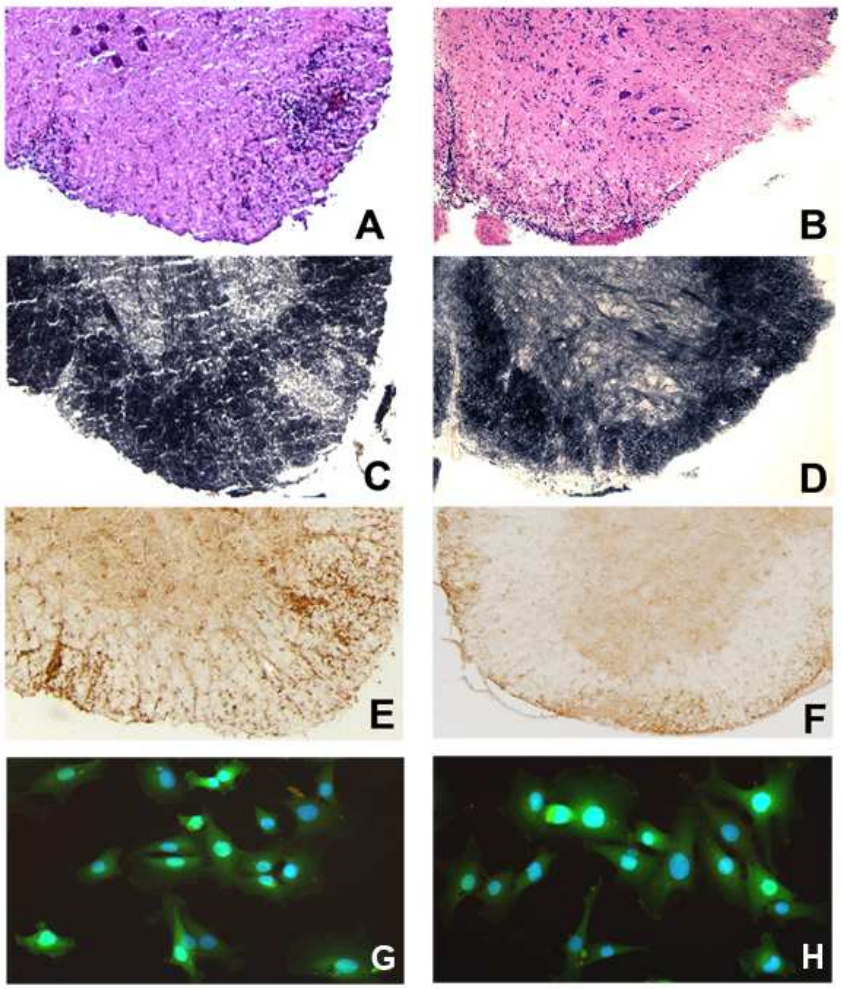

Bonetti et al

Supplementary Figure 2

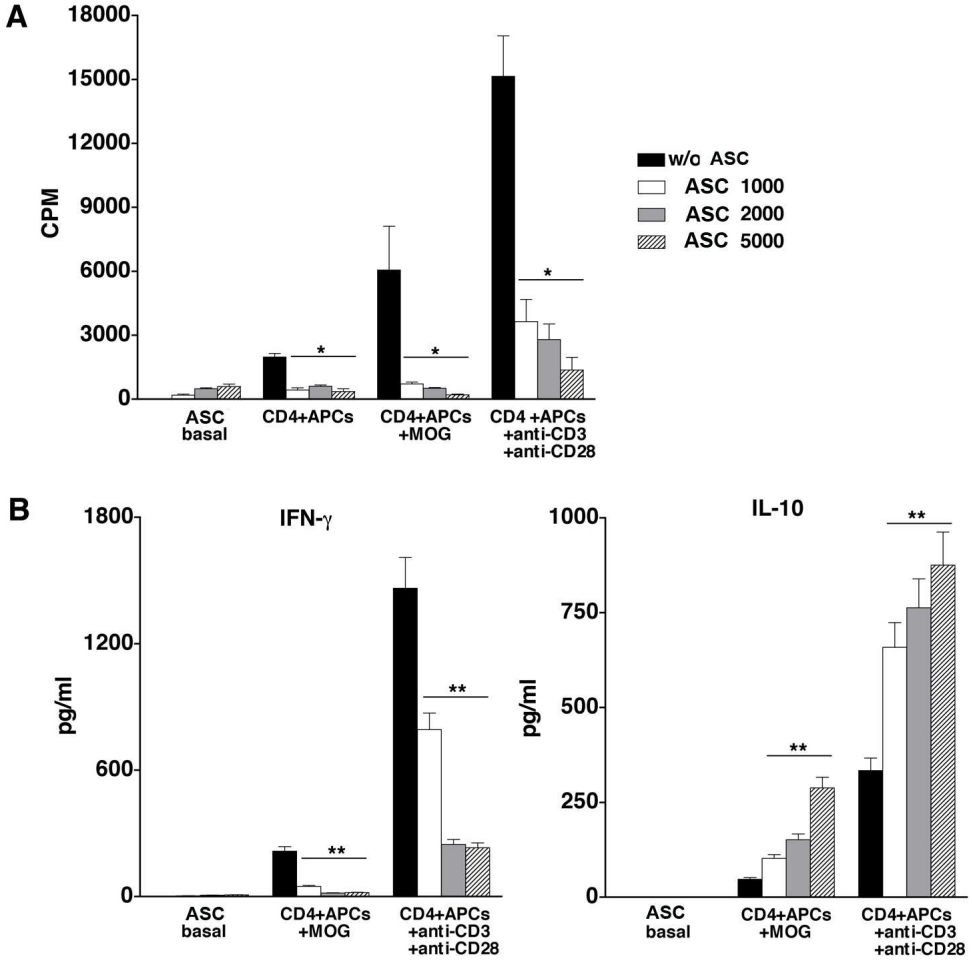

Bonetti et al Supplementary Figure 3

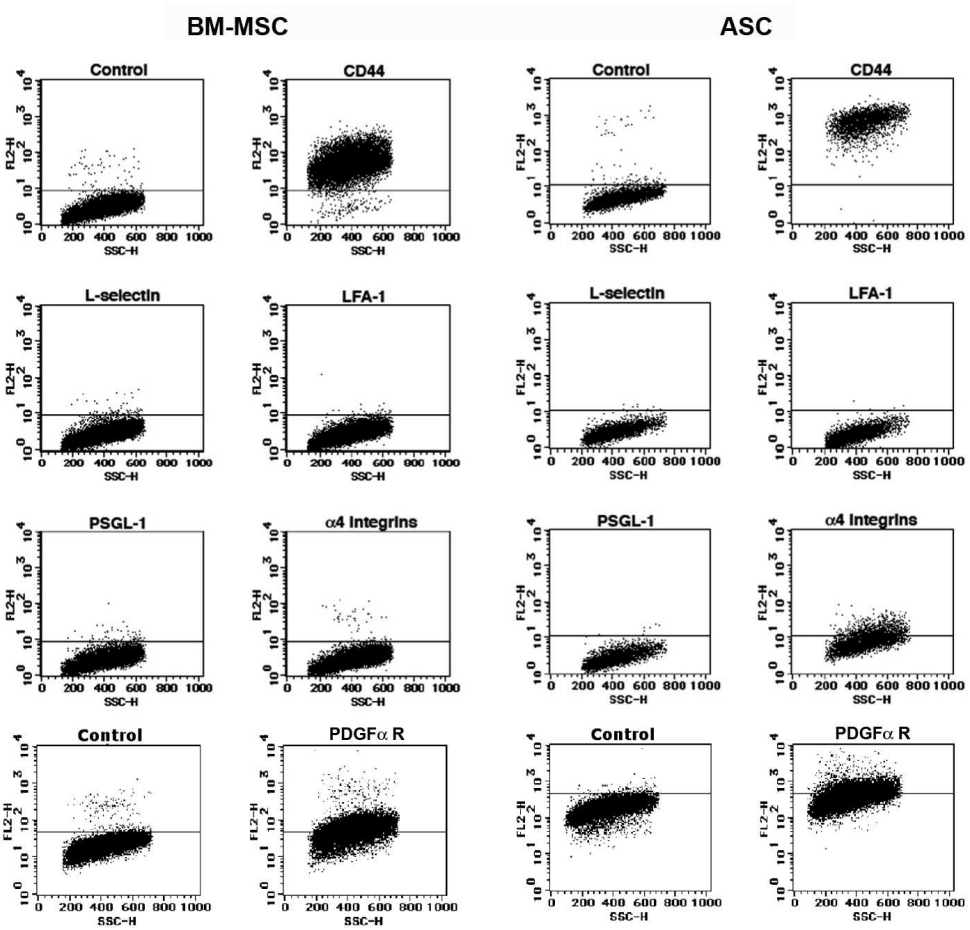

506x493mm (72 x 72 DPI)

Supplementary Figure 1. Neuropathological analysis confirms the beneficial effects of ASC in EAE. Hematoxylin and eosin (**A**, **B)** and Spielmeyer (**C, D**) stainings of lumbar spinal cords show reduction of inflammation and demyelination in ASC-treated mice (**B, D**), as compared to control mice (**A, C**). Quantification of these results is summarized in Table 1. **E**, **F**. Immunohistochemistry for CD3 T lymphocytes on serial sections show decreased number of inflammatory cells in EAE lesions from ASC-treated mice (**F**) in comparison to control mice (**E**). No evidence of anti-GFP Ig was observed in serum from control EAE (**G**) and ASC-treated (**H**) animals by testing respective sera for Ig autoreactivity to GFP^+ ASC cultures.

Supplementary Figure 2. Effect of ASC on the proliferation and cytokine production of encephalitogenic $CD4^+$ T-cells *in vitro*. A. $CD4^+$ cells isolated from draining lymph nodes of MOG_{35-55} immunized mice were re-stimulated *in vitro* for 3 days with MOG peptide or soluble anti-CD3/anti-CD28 mAbs, in the presence of irradiated APC and of 1,000, 2,000 or 5,000 ASC. Cell proliferation was assessed by [^{3}H]-thymidine incorporation and expressed as counts per minute (CPM). The co-culture with ASC induced a significant (p<0.005) and dose-dependent reduction of T cell proliferation after either antigen stimulation or CD3/CD28 activation, in comparison to control condition (w/o ASC). **B**. Secretion of cytokines (pg/ml) in supernatants by activated CD4 T cells was also significantly affected by co-culture with ASC, which induced a significant reduction of IFN-γ and an increase of IL-10 (p<0.02), as compared to the control condition (w/o ASC).

Supplementary Figure 3. A subset of ASC expresses α4 integrins and PDGFα R. Flow cytometry studies were performed in order to characterize on ASC and BM-MSC the expression of adhesion molecule repertoire, namely anti-leukocyte function-associated antigen (LFA-1), α4 integrins, L-selectin, P-selectin glycoprotein ligand (PSGL)-1, CD44.

The results show that about 20% of ASC, but not BM-MSC, express α4 integrin, suggesting that a sub-population of ASC might gain access to the inflamed brain. A subset of ASC (28% of the entire population examined) and about 60% of BM-MSC expressed PDGFα R on their surface in basal conditions.